The antitumor drugs trabectedin and lurbinectedin induce transcription-dependent replication stress and genome instability

Emanuela Tumini [1], Emilia Herrera-Moyano [1], Marta San Martín-Alonso [1], Sonia Barroso [1], Carlos M. Galmarini [2] and Andrés Aguilera [1] *

[1] *Centro Andaluz de Biología Molecular y Medicina Regenerativa-CABIMER, CSIC-Universidad Pablo de Olavide-Universidad de Sevilla, Av. Américo Vespucio 24, 41092 SEVILLE, Spain;* [2] *PharmaMar, Av. de los Reyes 1, 28770 Colmenar Viejo, Spain*

***Corresponding author:** Andrés Aguilera, Centro Andaluz de Biología Molecular y Medicina Regenerativa-CABIMER; Av. Américo Vespucio 24, 41092 SEVILLE, Spain. Phone: +34 954468372. E-mail: aguilo@us.es

Running title: ET743 and PM01183 and RNA-dependent DNA damage

Keywords

Trabectedin, lurbinectedin, R-loops, genome instability, cancer

Conflict of interests statement

Dr C.M. Galmarini is an employee and shareholder of PharmaMar. The remaining authors declare no conflict of interest.

ABSTRACT

R-loops are a major source of replication stress, DNA damage and genome instability, which are major hallmarks of cancer cells. Accordingly, growing evidence suggests that R-loops may also be related to cancer. Here we show that R-loops play an important role in the cellular response to trabectedin (ET743), an anticancer drug from marine origin and its derivative lurbinectedin (PM01183). Trabectedin and lurbinectedin induced RNA-DNA hybrid-dependent DNA damage in HeLa cells, causing replication impairment and genome instability. We also show that high levels of R-loops increase cell sensitivity to trabectedin. In addition, trabectedin led to transcription-dependent FANCD2 foci accumulation, which was suppressed by RNase H1 overexpression. In yeast, trabectedin and lurbinectedin increased the presence of Rad52 foci, a marker of DNA damage, in an R-loop-dependent manner. In addition to providing new insights into the mechanisms of action of these drugs, our study reveals that R-loops could be targeted by anticancer agents. Given the increasing evidence that R-loops occur all over the genome, the ability of lurbinectedin and trabectedin to act on them may contribute to enhance their efficacy, opening the possibility that R-loops might be a feature shared by specific cancers.

Implications: The data presented in this study provide the new concept that R-loops are important cellular factors that contribute to trabectedin and lurbinectedin anticancer activity.

Introduction

Cancer therapy greatly relies on the use of small molecules that directly perturb the DNA metabolism. Trabectedin (ET743) is one of such molecules. It has been initially derived from the sea squirt *Ecteinascidia turbinata* and is now produced synthetically, being currently employed in therapy of patients with advanced soft tissue sarcoma (1) and platinum-sensitive ovarian cancer (2). Different derivatives of trabectedin have been synthesized, among them lurbinectedin (PM01183), which is presently under evaluation in phase II and III clinical trials.

One of the most important features of the mechanism of action of trabectedin and lurbinectedin is their inhibitory effect on transcription of protein-coding genes that is mediated by different means. First, they preferentially bind to specific DNA triplets that are often present on transcription recognition sites. In this way they could directly prevent loading of transcription factors onto chromatin (3). Moreover, both drugs were shown to induce degradation of the RNA polymerase II (RNAPII) through the ubiquitin-proteasome pathway (4-8). Of note, these effects are also observed in tumor-associated macrophages (TAMs). Indeed, both drugs inhibit the transcription of selected cytokines (e.g. CCL2, IL6, IL8, PTX3) by TAMs abrogating their protumoral properties and modifying the tumor microenvironment (9, 10).

Tumor cells are commonly associated with genome instability. One important natural source of instability is represented by R-loops, a three-

stranded nucleic acid structure consisting of an RNA-DNA hybrid and the displaced single-stranded DNA of the original DNA duplex (11). This structure could fulfill physiological roles as it occurs during immunoglobulin class switching recombination, plasmid or mitochondrial DNA replication and transcription regulation. On the other hand, they are an important source of DNA damage, genome instability and replication stress, which relates R-loops with a number of neurodegenerative disorders and cancer (12, 13). Interestingly, the loss of function of the breast cancer susceptibility genes *BRCA1* and *BRCA2*, which have been shown to increase R-loops and R-loop-dependent DNA damage (14, 15), is also associated with an increased sensitivity to trabectedin (16). In a similar way, dysfunctions of the Fanconi anemia pathway that increased sensitivity to such agent (5) also cause accumulation of R-loops (17, 18).

In addition, there are some similarities between R-loops and trabectedin adducts worth being considered. The head-to-tail binding of three trabectedin molecules to three adjacent optimal DNA binding sites changes the DNA duplex conformation from the B-form to an intermediate between the A- and the B-form, which strongly resembles the conformation of an RNA-DNA hybrid (19). Moreover, R-loops that accumulate in the absence of the putative RNA-DNA helicases AQR or SETX require the action of Nucleotide Excision Repair (NER) to be processed into Double Strand Breaks (DSBs) (20) as well as trabectedin adducts (21).

For these reasons, in this study we have further explored the mechanism of action of trabectedin and lurbinectedin, in particular whether it could be partially mediated or affected by R-loops. We show that the DNA damage

and replicative stress caused by trabectedin and lurbinectedin is indeed partially dependent on R-loops, as demonstrated by molecular and genetic assays using both human cell lines and the yeast *Saccharomyces cerevisiae* as a model eukaryotic system. Our findings suggest that R-loops could be targets of anticancer agents and given the evidence that R-loops occur all over the genome (22), this opens the possibility that tumoral cells that accumulate R-loops may be more suitable for trabectedin and lurbinectedin treatment.

Materials and Methods

Cell culture and treatments

HeLa cells were purchased from ECACC (European Collection of Cell Cultures), HeLa-TR (24) and HeLa HB-GFP (14) were previously generated in our laboratory. All cell lines were maintained in DMEM medium, supplemented with 10% heat-inactivated fetal calf serum (FCS), cultured at 37ºC in a humidified atmosphere containing 5% CO_2 and routinely tested for Mycoplasma using MycoAlert Mycoplasma Detection Kit (Lonza). HeLa HB-GFP cells medium was supplemented with doxycycline at the final concentration of 2 μg/ml to induce HB-GFP expression. Specific genes were knocked down using ON-TARGET SMARTpool siRNA from Dharmacon. Transient transfection of siRNA was performed using DharmaFECT 1 (Dharmacon) according to the manufacturer's instructions. The following plasmids were used for transfection: pcDNA3 (Invitrogen) (RNH1-) and

pcDNA3-RNaseH1 (RNH1+), containing the full length RNase H1 cloned into pcDNA3 (23). Lipofectamine 2000 (Invitrogen, Carlsbad, CA) was used for plasmid transfection. Assays were performed 48h or 72h after transfection. Trabectedin (ET743) and lurbinectedin (PM01183) were provided from Pharmamar. Cordycepin (C3394) and Neocarzinostatin (N9162) were purchased from Sigma.

Single cell electrophoresis

Single cell electrophoresis or comet assays were performed as described using a commercial kit (Trevigen, Gaithersburg, MD, USA) following the manufacturer´s instructions. Comet tail moments were analyzed using Open Comet software. At least 100 cells were scored in each experiment to calculate the median of the tail moment, as reported (24).

Cell proliferation

HeLa cells were siRNA transfected to knock down the specified genes and plated in 96-well plate. Following 72 hours, cells were treated with increasing doses of trabectedin (ET743) for 24 hours and cell proliferation was measured by the WST-1 reagent (Roche) following the manufacture´s instructions. Absorbance was measured using microplate (ELISA) reader VARIOSKAN FLASH (Thermo) at 450 nm with a reference wavelength of 690 nm. Absorbance values were normalized to the value of the untreated and represented as arbitrary units (A.U.).

Antibodies

Antibodies anti-RNASEH1 (15606-1-AP) and anti-FANCD2 (sc-20022) anti-53BP1 (NB100-304) were purchased from Proteintech, Santa Cruz and Novus Biologicals, respectively. The S9.6 antibody was purified from the hybridoma cell line HB-8730.

Immunofluorescence and EdU labelling

Immunofluorescence was performed as previously described (25). Briefly, cells were fixed with 3.7% formaldehyde in PBS for 15 minutes, permeabilized with 0.5% Triton X-100 and blocked with 3% bovine serum albumin (BSA) in PBS for 1 hour. The coverslips were then incubated with primary antibodies diluted 1:500 in 3% BSA in PBS for 2 hours followed by 1 hour incubation with 1:1000 diluted secondary antibodies and nuclei counterstaining with 1 μg/ml DAPI in PBS. For FANCD2 immunolabelling, before fixation cells were pre-permeabilized with 0.25% Triton X-100 in PBS for 1 minute on ice. S9.6 immunofluorescence was performed as previously described (20). For the EdU labeling, cells were pulse-labeled with 10 μM EdU for 20 minutes before fixation. EdU staining was performed with a Click-iT EdU Alexa Fluor 555 Imaging kit (Invitrogen) according to manufacturer's instructions. Random images were acquired with a 63X or 40X objective and foci or nuclear intensity were scored using the MetaMorph software. At least 100 cells were scored for each condition.

DNA combing

DNA combing was performed as previously described (24). Briefly, DNA fibers were extracted from cells in agarose plugs immediately after CldU

labeling and were stretched on silanized coverslips. DNA molecules were counterstained with an autoanti-ssDNA antibody (DSHB, 1:500) and an anti-mouse IgG coupled to Alexa 647 (A21241, Molecular Probes, 1:50). CldU and IdU were detected with BU1/75 (AbCys, 1:20) and an anti-rat IgG coupled to Alexa 488 (A21470, Molecular Probes, 1:50) or B44 (Becton Dickinson, 1:20) anti-BrdU antibodies and an anti-mouse IgG coupled to Alexa 546 (A21123, Molecular Probes, 1:50), respectively. DNA fibers were analyzed on a Leica DM6000 microscope equipped with a DFC390 camera (Leica). Data acquisition was performed with LAS AF (Leica). Fork velocity was calculated as previously described (26). Replication asymmetry was calculated by dividing (longest green tract –shortest green tract) by the longest tract in divergent CIdU tracks.

Yeast 'halo' assay

Yeast cells of the wild-type W303 or the *rad52Δ* strains were plated in presence of 0.003% SDS in order to increase yeast cell permeability. Afterwards, paper filter disks were placed on the agar plates and 3 μL of increasing amounts of trabectedin or lurbinectedin (or DMSO as carrier control) were spotted onto them. After 3 to 6 days cells growth was monitored, plates were scanned and the diameter of the growth inhibition halo was measured.

Rad52 foci analysis in yeast cells

Wild-type W303 yeast cells were transformed in plates containing doxycycline (at the final concentration of 10 μg/ml in order to repress the

expression of ectopic RNase H1) with pWJ1344 plasmid coding the RAD52-YFP fusion protein (27) and with pCM189-RNH1 with the *RNH1* gene under the *tet* promoter (28) or the empty vector pCM189 (29). Cells were grown overnight with medium SC-L-U (Complete medium SC: 0.17% yeast nitrogen base and 0.5% ammonium sulfate, 2% glucose, supplemented with amino acids; –L and -U indicate the absence of leucine and uracil respectively) containing 0.003% SDS and without doxycyclin. Mid-log cultures overexpressing RNase H1 or not, were treated with increasing doses of trabectedin or lurbinectedin during 2 hours at 30ºC with 200 rpm shaking. Following fixation with 2.5% formaldehyde in 0.1M KHPO at pH 6.4 for 10 minutes, the cells were washed twice with KHPO 0.1M pH 6.6 and once with KHPO 0.1M pH 7.4. Cells were permeabilized with ethanol 80% for 10 minutes and after centrifugation were resuspended in water containing DAPI at the final concentration of 1 μg/ml to counterstain the nuclei. Rad52–YFP foci were scored in more than 200 nuclei from S-G2 mid-log cells, using a Leica DC 350F microscope.

Statistical analysis

Statistical significance was determined by t-tests or the Mann-Whitney test as specified. All tests performed were 2-tailed unless otherwise specified and three levels of statistical significance were considered: $*p \leq 0.05$, $**p \leq 0.01$ and $***p \leq 0.001$.

Results

Trabectedin and lurbinectedin treatment increase transcription-dependent DNA damage

Trabectedin and lurbinectedin covalently bind to DNA, physically impeding transcription and other DNA metabolic processes. To explore the possibility that the DNA adducts formed by these drugs could induce transcription-dependent genome instability, we analyzed DNA damage foci accumulation in HeLa cells in which transcription was abrogated by treatment with cordycepin, a potent transcription inhibitor that halts RNA chain elongation. HeLa cells treated during 4 hours with 25 nM of trabectedin or lurbinectedin accumulated 53BP1 foci, a DSB marker (Fig. 1 a). However, when transcription was previously shut off with cordycepin (added 1 hour earlier), 53BP1 foci were significantly reduced, suggesting an important role of transcription in the mechanism of action of these drugs.

Next, we assayed whether RNA-DNA hybrids could be involved in the transcription-dependent DNA damage observed. Indeed, overexpression of RNase H1, which removes the RNA moiety of the hybrids, partially reduced the 53BP1 foci observed after trabectedin treatment, suggesting that part of the role of transcription in the mechanism of action of these drugs was associated with R-loops (Supplementary Fig. S1). In this case we exposed cells to a lower dose of trabectedin for longer (10nM during 6 hours) to better see the increase of 53BP1 foci. This longer treatment was not possible with cordycepin-mediated transcription shut off.

Provided the known negative effect of transcription and RNA-DNA hybrids on replication fork (RF) progression we decided to analyze the

accumulation of FANCD2 foci, a central player of the Fanconi Anemia (FA) DNA repair pathway, as a way to measure repair events occurring at potential stalled forks. FA is a DNA repair pathway that works on stalled RFs and cells deficient in this pathway have also been shown to be more sensitive to trabectedin (5). The experiment was performed as described above for 53BP1 foci. Trabectedin and lurbinectedin caused a significant increase of FANCD2 foci that was completely reversed by cordycepin treatment (Fig. 1b), suggesting a key role of these drugs in transcription-replication (T-R) conflicts. Since both drugs caused very similar phenotypes, consistent with an expected common mechanism of action, we focused the rest of the study mainly on trabectedin.

FANCD2 foci accumulation approximately doubled after a longer exposure to trabectedin at lower dose and this increase was entirely rescued by RNase H1 overexpression (Fig. 1c). To assure that this suppression by RNase H1 was specific for trabectedin, we analyzed the effect of a different and well-establish genotoxic and antitumoral drug, neocarzinostatin (30), and we found that it also increased FANCD2 foci but this phenotype was not suppressed by RNase H1 overexpression (Supplementary Fig. S2). Given the observed connection of RNA-DNA hybrids and DNA damage with trabectedin and lurbinectedin treatment, we tested directly for the presence of RNA-DNA hybrids using the S9.6 antibody, which specifically recognizes these structures, by *in situ* immunofluorescence (IF). As can be seen in Supplementary Fig. S3, trabectedin and lurbinectedin did not cause a significant increase in the nuclear intensity of the S9.6 signal. Since these drugs significantly decrease transcription and therefore the overall RNA

levels (8, 31) it is unlikely that they concomitantly increase R-loop levels. Nonetheless, they could act by exacerbating their impact on replication and genome integrity. Consistently, both drugs affected nucleolus integrity, as deduced from a perturbed localization of the nucleolar marker nucleolin and by a smaller or fragmented appearance of nucleoli detected with the S9.6 antibody.

Trabectedin enhances R-loop-dependent replication impairment

Trabectedin directly interacts with DNA, forming adducts and producing distortions of the double helix. Since R-loops impair replication progression (32-36) we analyzed the impact of trabectedin on DNA replication and whether this would be associated with the presence of RNA-DNA hybrids. For this, we first assessed DNA replication levels after trabectedin treatment, by measuring the amount of incorporated EdU, a thymidine analog. Trabectedin treatment strongly affected the rate of DNA synthesis in HeLa cells, leading to lower levels of EdU incorporation compared to untreated cells (Fig. 2a). However, the percentage of cells in S phase (EdU-incorporating cells) was not affected (Supplementary Fig. S4a). Importantly, overexpression of RNase H1, which by itself caused a slight decrease in EdU incorporation, partially rescued the phenotype of reduced DNA synthesis (Fig. 2a).

Next, we used DNA combing to check for impairment of replication fork progression in single molecules. Using low trabectedin concentrations at which the replication fork velocity was not perturbed, the drug caused an increase in fork stalling, as determined by fork asymmetry, which was

significantly higher in trabectedin-treated versus non-treated cells (Fig. 2b). To know whether this effect was dependent on transcription, required for the co-transcriptional formation of RNA-DNA hybrids, we inhibited transcription using cordycepin. With this approach, all cells were exposed to the same treatment, something that was not possible after transfection with an RNase H1-overexpressing plasmid. We observed that treatment of cells with the transcription inhibitor cordycepin abolished the difference in fork asymmetry between trabectedin-treated and untreated samples. This result suggests that fork-stalling caused by trabectedin is linked to transcription. Inhibition of transcription by cordycepin was detrimental for replication at higher doses of trabectedin, which *per se* provoked a reduction in the replication rate (Supplementary Fig. S4b). Thus, it was not surprising that the concomitant treatment with the two chemicals reduced further the DNA replication rate as assessed by EdU incorporation. However, since trabectedin can also inhibit transcription (31), it is possible that the effect on DNA replication has multiple causes that would require further investigation.

Based on these observations, we infer that the replication obstacles posed by trabectedin treatment are partially dependent on RNA-DNA hybrids.

RNA-DNA hybrid-accumulating cells are hyper-sensitive to trabectedin

To better establish a functional link between RNA-DNA hybrids and trabectedin, we assayed the sensitivity to trabectedin of cells in which RNA-DNA hybrids were stabilized by a hybrid-binding protein. For this purpose we took advantage of a stable cell line that expresses the chimeric protein HB-

GFP, a fusion protein constituted by the hybrid binding (HB) domain of the RNase H1 enzyme and the green fluorescent protein (GFP). Under these conditions RNA-DNA hybrids are likely “stabilized” by the binding of the HB domain, thus retaining the R-loops in the cell, consistent with previously reported results from BRCA2-depleted cells (14). Interestingly, cells expressing the HB-GFP fusion protein were more sensitive to trabectedin as assessed by cell proliferation assays (Fig. 3, left panel), suggesting that cells with higher levels of R-loops can be made more susceptible to this anticancer agent. We next knocked down two cellular factors, THOC1 and BRCA2, previously shown to enhance RNA-DNA hybrids by either preventing their formation or by promoting their removal. Depletion of any of the two genes is associated with an increase in RNA-DNA hybrids formation (14). The lack of BRCA2 or THOC1 increased cellular sensitivity to trabectedin both in the absence of HB-GFP and in cells expressing HB-GFP (Fig. 3, middle and right panel), having THOC1 depletion a stronger effect.

Trabectedin and lurbinectedin induce DNA breaks that are partially mediated by RNA-DNA hybrids in human cells.

Next, we analyzed the effect of trabectedin treatment in cell proliferation and genome integrity in human cells in relation to R-loop accumulation. For this, HeLa cells were first transfected with a plasmid that leads to the overexpression of RNase H1 before being treated with trabectedin or lurbinectedin and analyzed by alkaline single cell electrophoresis (comet assay) for the accumulation of DNA breaks. As shown in Fig. 4, trabectedin and lurbinectedin increased DNA breaks, as expected. However, when cells

overexpressed RNase H1, breaks were significantly reduced in cells treated with 50 nM lurbinectedin for 2 hour. We evaluated γH2AX foci formation, a molecular marker that in addition to DNA damage is also associated with replicative stress signaling. Trabectedin treatment increased γH2AX foci accumulation (Supplementary Fig. S5a). In this case, however, RNase H1 treatment increased further the γH2AX foci, suggesting that a double treatment with trabectedin and RNase H1 leads to an additive replicative stress and DNA damage. Indeed, RNA-DNA hybrids are also important intermediates of normal DNA replication (for Okazaki fragment synthesis) and, consistently, a clonogenic assay revealed that survival of cells overexpressing RNase H1 at the time of treatment with increasing doses of trabectedin was reduced (Supplementary Fig. S5b).

The RNA-DNA hybrid-dependent genome instability associated with trabectedin and lurbinectedin is evolutionary conserved.

To investigate whether trabectedin and lurbinectedin interact with RNA-DNA hybrids regardless of cell type and organism as a way to confirm that they target directly DNA metabolism, we asked whether similar DDR phenotypes could be reproduced in the eukaryotic model organism *Saccharomyces cerevisiae.* For this we first analyzed the effect of trabectedin. Replication impairment causes genome instability and Rad52 is used as a marker to detect instability in the form of the accumulation of DNA damage. To assess sensitivity to trabectedin and lurbinectedin, we used the "halo" assay. Different yeast strains were homogenously plated on YEPD-rich medium plates, and then Whatman-paper disks soaked with increasing

concentrations of the tested drug were placed on top of the plate. After growth, halos of growth inhibition around the disks were formed with a diameter that correlates with the levels of toxicity of the drug. As can be seen in Fig. 5a, increasing concentrations of trabectedin lead to increased yeast sensitivity, as detected by the size of the halo of growth inhibition around the trabectedin spot. Importantly, this halo was largely increased in *rad52Δ* yeast strains inactivated for homologous recombination DSB repair in comparison with the wild-type strain, even at concentrations at which trabectedin had no effect on wild-type cells (Fig. 5a). This result suggests that recombinogenic DNA breaks accumulated after trabectedin treatment, consistent with previous reports (21). To confirm this, we analyzed recombinogenic DSBs by Rad52 foci, used as a way to detect DSB repair centers (27). Consistently, trabectedin caused a significant increase of Rad52 foci. Cells treated with 250 μM trabectedin, showed a 3-fold increase in the percentage of cells with Rad52 foci compared to the untreated control (Fig. 5b). To assay whether Rad52 foci were dependent on RNA-DNA hybrids, RNAse H1 was overexpressed in yeast cells by transformation with an RNase H1-overexpressing plasmid. Notably, the increase in Rad52 foci was suppressed by RNase H1 overexpression (Fig. 5b and Supplementary Fig. S6a). These results indicate that trabectedin-induced breaks are linked to the accumulation of RNA-DNA hybrids also in yeast cells.

Next, we assayed the effect of lurbinectedin on cell growth and genome instability using the assays described above for trabectedin. As can be seen in Fig. 5c, lurbinectedin affected yeast growth as determined by the size of the growth inhibition halo formed around the increasing concentrations of the

chemical spotted on Whatman filter papers. Again, this effect was significantly enhanced in *rad52*Δ strains, consistent with the idea that cell growth was impaired due to the accumulation of unrepaired DSBs. Accordingly, lurbinectedin treatment caused a 2-3-fold increase of cells with Rad52 foci compared to untreated cells and this phenotype was fully suppressed by RNase H1 overexpression (Fig. 5d and Supplementary Fig. S6a). The decreased amount of Rad52 foci after overexpression of RNase H1 in trabectedin- or lurbinectedin-treated cells, was not due to the reduction of the protein levels, as confirmed by western blot (Supplementary Fig. S6b).

Consequently, lurbinectedin, as well as trabectedin, caused R-loop dependent genome instability both in yeast and in human cells. This finding suggests that their action is most likely common to many different cell types, since they target molecular pathways that are well conserved across evolution.

Discussion

Increasing evidence points out the role of RNA-DNA hybrids in the boost of genome instability and replication stress that are major hallmarks of cancer cells. This opens the possibility that such hybrids could occur at high levels in some tumor cells and consequently could be used as therapeutic targets. For this reason, it is of growing importance to address the relationship between R-loops and the action of anticancer agents. Trabectedin and lurbinectedin are two powerful drugs used in cancer treatment whose ability to block cell proliferation is linked to its potential to

cause DNA breaks and inhibit transcription. In this study, we show that trabectedin and lurbinectedin activities are favored by transcription and, at least partially, they might be enhanced by R-loops. Trabectedin and lurbinectedin treatment enhanced transcription-dependent genome instability and replication stress (Figs. 1 and 2). Exposure to trabectedin or lurbinectedin did not cause a global increase in R-loops as assayed by S9.6 immunofluorescence (Supplementary Fig. S3). However, these drugs caused genome instability and replicative stress that were dependent on transcription and RNA-DNA hybrids both in yeast and human cells. These findings suggest that trabectedin and lurbinectedin toxicity is higher at sites undergoing active transcription and R-loop accumulation.

It was previously demonstrated that trabectedin and lurbinectedin directly bind DNA, forming adducts (6) and distort the double helix. Here we showed that these DNA adducts compromise replication fork progression; indeed, we found that trabectedin caused a profound impairment of DNA synthesis (Fig. 2a). To some extent, we can attribute this effect to R-loop formation, because RNase H1 overexpression partially suppressed this DNA synthesis defect. RNase H1 specifically cleaves the RNA strand of RNA-DNA hybrids therefore, overexpression of this endoribonuclease counteracts the accumulation of RNA-DNA hybrids. However, the rescue of the EdU incorporation defect by RNase H1 overexpression was mild, which suggests that only a subset of the trabectedin-induced replicative problems were mediated by RNA-DNA hybrids. Analysis of DNA replication at the single molecule level by DNA combing revealed that transcription inhibition with cordycepin reduces the increase in fork asymmetry provoked by trabectedin

exposure (Fig. 2b), consistent with the conclusion that R-loops contribute to fork stalling in trabectedin treated cells. In any case, we cannot exclude the possibility that the inhibition of transcription by trabectedin could contribute to RF asymmetry.

R-loop-dependent replication problems caused by trabectedin are possibly counteracted by the Fanconi Anemia (FA) pathway. The FA pathway has a key role in balancing replication stress, in particular when inter-strand crosslinking agents such as Mitomycin C (MMC) cause replication fork blockage (37) and has been shown to limit R-loop accumulation and R-loop-dependent genome instability (17, 18). Interestingly, FA is critical for the integrity of common fragile sites (CFSs), since FANCD2, a central player of the FA pathway, is required for a safe replication through R-loop-accumulating CFSs (38). Here, we found an increased accumulation of FANCD2 foci after trabectedin treatment that, importantly, was fully rescued by RNase H1 overexpression (Fig. 1c). This phenotype was different to that caused by other genotoxic agents. Thus, contrary to trabectedin, overexpression of RNase H1 in cells treated with the radiomimetic agent neocarzinostatin (NCZ) exacerbated FANCD2 foci accumulation (Supplementary Fig. S2). This may be explained if FANCD2 foci induced by NCZ are not RNA-DNA hybrid-dependent, and RNase H1 overexpression causes an additional type of replication stress. This finding adds further support to the conclusion that trabectedin has a prominent and specific action on R-loops where it preferentially causes DNA damage and breaks able to block replication fork progression. Consistently, using a cell line system where R-loops were stabilized by the ectopic expression of the

476 RNA-DNA hybrid binding domain of the RNase H1 enzyme fused to GFP,
477 and additionally increasing the basal levels of R-loop through the siRNA-
478 mediated depletion of THOC1 or BRCA2, we determined that cells with
479 higher levels of R-loops were more sensitive to trabectedin treatment (Fig.
480 3).

481 Importantly, we were able to recapitulate the phenotype of R-loop-
482 dependent genome instability caused by trabectedin and lurbinectedin in
483 yeast cells. Rad52 foci induced after treatment of either trabectedin or
484 lurbinectedin were rescued by RNase H1 overexpression (Fig. 5). This result
485 strongly suggests that the preferred action of these anti-tumoral agents on
486 DNA is independent of the eukaryotic system or cell type, arguing strongly in
487 favor of a preferential action on the R-loop-containing chromatin. In HeLa
488 cells exposed to these agents, the RNA-DNA hybrid-dependent DNA
489 damage phenotype was not so clear as it was in yeast cells. However, we
490 were able to show by comet assay and 53BP1 immunofluorescence that the
491 DNA damage induced by trabectedin or lurbinectedin was partially rescued
492 by RNase H1 overexpression (Fig. 4 and Supplementary Fig. S1). Besides,
493 we found that γH2AX foci accumulation after trabectedin treatment was
494 further increased in cells overexpressing RNase H1 (Supplementary Fig.
495 S5a). However, even if phosphorylated γH2AX on Ser139 is used as a DSB
496 marker, it also denotes replication stress, since it is extended through a large
497 chromatin domain as an early response to replication fork stalling in an ATR-
498 dependent process (39). RNase H1 overexpression could cause replication
499 stress and instability, likely because it hampers replication by altering
500 Okazaki fragment dynamics. Accordingly, DNA synthesis was impaired in

cells overexpressing RNase H1 (Fig. 2a). The double treatment with RNase H1 overexpression and trabectedin might have an additive effect by their impact on replication, enhancing the probability of ssDNA gaps or breaks that would lead to increased cell death (Supplementary Fig. S5b).

The novel finding of an interplay between R-loops and trabectedin in genome instability induction, is of particular interest because it could be exploited for cancer cells in which R-loops might be a common feature. The observation that trabectedin toxicity is augmented by the dysfunction in pathway that have been shown to protect both from cancer and from R-loops accumulation, such as the Fanconi anemia pathway and the *BRCA1* and *BRCA2* tumor suppressor genes (14, 15, 17, 18), supports the idea that R-loops might be a hallmark of specific types of cancer (40). It has been shown that cancer patients with *BRCA* mutations exhibit improved clinical response to trabectedin (16). It would be interesting in the future to check if R-loops are increased in tumoral cells derived from such patients to strengthen our hypothesis that a subset of tumors characterized by an higher accumulation of R-loops are more suitable to be treated with trabectedin.

Disclosure of Potential Conflicts of interests

Dr C.M. Galmarini is an employee and shareholder of PharmaMar. The remaining authors declare no conflict of interest.

Authors' contributions

E.T., C.M.G. and A.A. conceived and designed the experiments; E.T., E.H.M., S.B. and M.S.M.A. performed the experiments; E.T., E.H.M.,

M.S.M.A., S.B. and A.A. analyzed the data; E.T., C.M.G. and A.A. wrote the manuscript.

Acknowledgments

We thank Hélène Gaillard and Oksana Brehey for assistance in setting up yeast experiments.

This work was supported with funding by the European Research Council (ERC2014 AdG669898 TARLOOP), the Spanish Ministry of Economy and Competitiveness (BFU2016-75058-P), the European Union (FEDER) (BFU2016-75058-P) and PharmaMar (PRJ201402213).

References

1. Gordon EM, Sankhala KK, Chawla N, Chawla SP. Trabectedin for Soft Tissue Sarcoma: Current Status and Future Perspectives. Adv Ther. 2016;**33**:1055-1071.

2. Teplinsky E, Herzog TJ. The efficacy of trabectedin in treating ovarian cancer. Expert Opin Pharmacother. 2017;**18**:313-323.

3. Minuzzo M, Marchini S, Broggini M, Faircloth G, D'Incalci M, Mantovani R. Interference of transcriptional activation by the antineoplastic drug ecteinascidin-743. Proc Natl Acad Sci U S A. 2000;**97**:6780-6784.

4. Aune GJ, Takagi K, Sordet O, Guirouilh-Barbat J, Antony S, Bohr VA, et al. Von Hippel-Lindau-coupled and transcription-coupled nucleotide excision repair-dependent degradation of RNA polymerase II in response to trabectedin. Clin Cancer Res. 2008;**14**:6449-6455.

5. Casado JA, Rio P, Marco E, Garcia-Hernandez V, Domingo A, Perez L, et al. Relevance of the Fanconi anemia pathway in the response of human cells to trabectedin. Mol Cancer Ther. 2008;**7**:1309-1318.

6. Leal JF, Martinez-Diez M, Garcia-Hernandez V, Moneo V, Domingo A, Bueren-Calabuig JA, et al. PM01183, a new DNA minor groove covalent binder with potent in vitro and in vivo anti-tumour activity. Br J Pharmacol. 2010;**161**:1099-1110.

7. Romano M, Frapolli R, Zangarini M, Bello E, Porcu L, Galmarini CM, et al. Comparison of in vitro and in vivo biological effects of trabectedin, lurbinectedin (PM01183) and Zalypsis(R) (PM00104). Int J Cancer. 2013;**133**:2024-2033.

8. Santamaria Nunez G, Robles CM, Giraudon C, Martinez-Leal JF, Compe E, Coin F, et al. Lurbinectedin Specifically Triggers the Degradation of Phosphorylated RNA Polymerase II and the Formation of DNA Breaks in Cancer Cells. Mol Cancer Ther. 2016;**15**:2399-2412.

9. Germano G, Frapolli R, Belgiovine C, Anselmo A, Pesce S, Liguori M, et al. Role of macrophage targeting in the antitumor activity of trabectedin. Cancer Cell. 2013;**23**:249-262.

10. Belgiovine C, Bello E, Liguori M, Craparotta I, Mannarino L, Paracchini L, et al. Lurbinectedin reduces tumour-associated macrophages and the

574 inflammatory tumour microenvironment in preclinical models. Br J Cancer.
575 2017;**117**:628-638.
576 11. Aguilera A, Garcia-Muse T. Causes of genome instability. Annu Rev
577 Genet. 2013;**47**:1-32.
578 12. Santos-Pereira JM, Aguilera A. R loops: new modulators of genome
579 dynamics and function. Nat Rev Genet. 2015;**16**:583-597.
580 13. Skourti-Stathaki K, Proudfoot NJ. A double-edged sword: R loops as
581 threats to genome integrity and powerful regulators of gene expression. Genes
582 Dev. 2014;**28**:1384-1396.
583 14. Bhatia V, Barroso SI, Garcia-Rubio ML, Tumini E, Herrera-Moyano E,
584 Aguilera A. BRCA2 prevents R-loop accumulation and associates with TREX-2
585 mRNA export factor PCID2. Nature. 2014;**511**:362-365.
586 15. Hill SJ, Rolland T, Adelmant G, Xia X, Owen MS, Dricot A, et al.
587 Systematic screening reveals a role for BRCA1 in the response to transcription-
588 associated DNA damage. Genes Dev. 2014;**28**:1957-1975.
589 16. Monk BJ, Lorusso D, Italiano A, Kaye SB, Aracil M, Tanovic A, et al.
590 Trabectedin as a chemotherapy option for patients with BRCA deficiency.
591 Cancer Treat Rev. 2016;**50**:175-182.
592 17. Garcia-Rubio ML, Perez-Calero C, Barroso SI, Tumini E, Herrera-
593 Moyano E, Rosado IV, et al. The Fanconi Anemia Pathway Protects Genome
594 Integrity from R-loops. PLoS Genet. 2015;**11**:e1005674.
595 18. Schwab RA, Nieminuszczy J, Shah F, Langton J, Lopez Martinez D,
596 Liang CC, et al. The Fanconi Anemia Pathway Maintains Genome Stability by
597 Coordinating Replication and Transcription. Mol Cell. 2015;**60**:351-361.

19. Marco E, Garcia-Nieto R, Mendieta J, Manzanares I, Cuevas C, Gago F. A 3.(ET743)-DNA complex that both resembles an RNA-DNA hybrid and mimicks zinc finger-induced DNA structural distortions. J Med Chem. 2002;**45**:871-880.

20. Sollier J, Stork CT, Garcia-Rubio ML, Paulsen RD, Aguilera A, Cimprich KA. Transcription-coupled nucleotide excision repair factors promote R-loop-induced genome instability. Mol Cell. 2014;**56**:777-785.

21. Herrero AB, Martin-Castellanos C, Marco E, Gago F, Moreno S. Cross-talk between nucleotide excision and homologous recombination DNA repair pathways in the mechanism of action of antitumor trabectedin. Cancer Res. 2006;**66**:8155-8162.

22. Wongsurawat T, Jenjaroenpun P, Kwoh CK, Kuznetsov V. Quantitative model of R-loop forming structures reveals a novel level of RNA-DNA interactome complexity. Nucleic Acids Res. 2012;**40**:e16.

23. ten Asbroek AL, van Groenigen M, Nooij M, Baas F. The involvement of human ribonucleases H1 and H2 in the variation of response of cells to antisense phosphorothioate oligonucleotides. Eur J Biochem. 2002;**269**:583-592.

24. Dominguez-Sanchez MS, Barroso S, Gomez-Gonzalez B, Luna R, Aguilera A. Genome instability and transcription elongation impairment in human cells depleted of THO/TREX. PLoS Genet. 2011;**7**:e1002386.

25. Tumini E, Barroso S, Calero CP, Aguilera A. Roles of human POLD1 and POLD3 in genome stability. Sci Rep. 2016;**6**:38873.

621 26. Bianco JN, Poli J, Saksouk J, Bacal J, Silva MJ, Yoshida K, et al.
622 Analysis of DNA replication profiles in budding yeast and mammalian cells
623 using DNA combing. Methods. 2012;**57**:149-157.
624 27. Lisby M, Rothstein R, Mortensen UH. Rad52 forms DNA repair and
625 recombination centers during S phase. Proc Natl Acad Sci U S A.
626 2001;**98**:8276-8282.
627 28. Castellano-Pozo M, Santos-Pereira JM, Rondon AG, Barroso S, Andujar
628 E, Perez-Alegre M, et al. R loops are linked to histone H3 S10 phosphorylation
629 and chromatin condensation. Mol Cell. 2013;**52**:583-590.
630 29. Gari E, Piedrafita L, Aldea M, Herrero E. A set of vectors with a
631 tetracycline-regulatable promoter system for modulated gene expression in
632 Saccharomyces cerevisiae. Yeast. 1997;**13**:837-848.
633 30. Kim KH, Kwon BM, Myers AG, Rees DC. Crystal structure of
634 neocarzinostatin, an antitumor protein-chromophore complex. Science.
635 1993;**262**:1042-1046.
636 31. D'Incalci M, Galmarini CM. A review of trabectedin (ET-743): a unique
637 mechanism of action. Mol Cancer Ther. 2010;**9**:2157-2163.
638 32. Gan W, Guan Z, Liu J, Gui T, Shen K, Manley JL, et al. R-loop-mediated
639 genomic instability is caused by impairment of replication fork progression.
640 Genes Dev. 2011;**25**:2041-2056.
641 33. Wellinger RE, Prado F, Aguilera A. Replication fork progression is
642 impaired by transcription in hyperrecombinant yeast cells lacking a functional
643 THO complex. Mol Cell Biol. 2006;**26**:3327-3334.

644 34. Salas-Armenteros I, Perez-Calero C, Bayona-Feliu A, Tumini E, Luna R,
645 Aguilera A. Human THO-Sin3A interaction reveals new mechanisms to prevent
646 R-loops that cause genome instability. EMBO J. 2017;**36**:3532-3547.
647 35. Hamperl S, Bocek MJ, Saldivar JC, Swigut T, Cimprich KA.
648 Transcription-Replication Conflict Orientation Modulates R-Loop Levels and
649 Activates Distinct DNA Damage Responses. Cell. 2017;**170**:774-786 e719.
650 36. Lang KS, Hall AN, Merrikh CN, Ragheb M, Tabakh H, Pollock AJ, et al.
651 Replication-Transcription Conflicts Generate R-Loops that Orchestrate Bacterial
652 Stress Survival and Pathogenesis. Cell. 2017;**170**:787-799 e718.
653 37. Ceccaldi R, Sarangi P, D'Andrea AD. The Fanconi anaemia pathway:
654 new players and new functions. Nat Rev Mol Cell Biol. 2016;**17**:337-349.
655 38. Madireddy A, Kosiyatrakul ST, Boisvert RA, Herrera-Moyano E, Garcia-
656 Rubio ML, Gerhardt J, et al. FANCD2 Facilitates Replication through Common
657 Fragile Sites. Mol Cell. 2016;**64**:388-404.
658 39. Sirbu BM, Couch FB, Feigerle JT, Bhaskara S, Hiebert SW, Cortez D.
659 Analysis of protein dynamics at active, stalled, and collapsed replication forks.
660 Genes Dev. 2011;**25**:1320-1327.
661 40. Gaillard H, Garcia-Muse T, Aguilera A. Replication stress and cancer.
662 Nat Rev Cancer. 2015;**15**:276-289.

663

FIGURE LEGENDS

Fig. 1. Trabectedin and lurbinectedin treatment increased transcription-dependent 53BP1 and FANCD2 foci

(**a** and **b**) Immunodetection of 53BP1 and FANCD2 foci in HeLa cells treated with trabectedin (ET743 or ET), lurbinectedin (PM01183 or PM) or left untreated (Unt) as indicated. Cells were or were not pretreated with cordycepin 50 μM (CORD- or CORD+) during 1 hour and during the following 4 hours of treatment. Representative images and quantification are shown. Bars represent the averages ± SEM of the percentage of cells with more than 5 foci from at least 3 independent experiments. (**c**) HeLa cells were transfected with the RNase H1 overexpression plasmid (RNH1+) or with the empty vector (RNH1-). Following 24 hours after transfection cells were treated with trabectedin (ET743) as indicated. After the incubation with ET743 cells were fixed and immunodetection of FANCD2 was performed. Representative images and quantification of cells with more than 5 FANCD2 foci in cells positive for RNase H1 overexpression are shown. Bars represent the averages ± SEM of the percentage of cells with more than 5 foci from 5 independent experiments. Statistical significance was assessed by Student's t-test.

Fig. 2. Trabectedin treatment caused R-loop dependent replication impairment

(**a**) HeLa cells were transfected with a plasmid built to overexpress RNase H1 (RNH1+) or with the empty vector (RNH1-). Following 24 hours after transfection cells were treated with trabectedin (ET743) as indicated and pulse

689 labelled with EdU before fixation. Representative images from the cells labelled
690 for EdU and RNase H1. Distribution of EdU nuclear intensity in cells positive for
691 EdU (in RNH1- and in RNH1+ cells) and for RNase H1 overexpression (in
692 RNH1+ cells) presented by a scatter dot plot where the median value is shown.
693 The data from three independent experiments were pulled together. Differences
694 between distributions were assessed by the Mann-Whitney test. (**b**) Outline of
695 the experimental procedure followed before harvesting and processing HeLa
696 cells for DNA combing. Distribution of replication fork velocity and asymmetry
697 are presented by a scatter dot plot where the median value is shown. “Cord”
698 indicates cordycepin. The data from four or two independent experiments were
699 pulled together for fork velocity and asymmetry, respectively. Differences
700 between distributions were assessed by the Mann-Whitney test.
701
702 **Fig. 3. HB-GFP cells showed increased sensitivity to trabectedin treatment**
703 HB-GFP cells (HB-GFP+) expressing the fusion protein HB-GFP or the parental
704 cell line (HB-GFP-) were knocked down for the specified genes for 72 hours.
705 After treatment with increasing doses of trabectedin (ET743) for 24 hours cell
706 proliferation was measured by the WST-1 reagent. The graph shows the
707 relative values of cell proliferation referred to the untreated sample at increasing
708 doses of trabectedin. Averages ± SEM from 10 independent experiments is
709 presented. Statistical significance was assessed by paired t-test comparing for
710 each siRNA the parental cells with the HB-GFP-expressing cell line. In the
711 central and left graphs the dotted grey line represents the parental cells
712 transfected by siC.
713

Fig. 4. Trabectedin and lurbinectedin caused R-loop dependent DNA damage

HeLa cells were transfected with the RNase H1 overexpression plasmid (RNH1+) or with the empty vector (RNH1-). Following 48 hours after transfection cells were treated with trabectedin (ET743) (**a**) or lurbinectedin (PM01183) (**b**) as indicated and DNA damage levels were measured. Representative images from alkaline comet assays and quantification of the tail moment are shown. Bars represent the averages ± SEM (Standard Error of the Mean) of the median from at least three independent experiments. Statistical significance was assessed by the one-tailed Mann-Whitney test.

Fig. 5. Trabectedin or lurbinectedin treatment caused R-loop dependent genome instability in yeast cells

(**a**) Representative images of halo assay performed in W303 and *rad52Δ* yeast cells and quantification of the inhibition halo diameter after the indicated trabectedin (ET743) treatments. Bars represent the averages ± SEM from 4 independent experiments. Statistical significance was assessed by Student's t-test. (**b**) Yeast cells W303 were transfected with Rad52-GFP plasmid and the RNase H1 overexpression plasmid (RNH1+) or with the empty vector (RNH1-) and treated with increasing amount of trabectedin. Bars represent the averages ± SEM of the percentage of cells with one or more Rad52 foci from 3 independent experiments. Statistical significance was assessed by Student's t-test. (**c**) Representative image of halo assay performed in W303 and *rad52Δ* yeast cells and quantification of the inhibition halo diameter after the indicated lurbinectedin (PM01183) treatments. Bars represent the averages ± SEM from

739 4 independent experiments. Statistical significance was assessed by Student's
740 t-test. (**d**) Yeast cells W303 were transfected with Rad52-GFP plasmid and
741 RNase H1 overexpression plasmid (RNH1+) or with the empty vector (RNH1-)
742 and treated with increasing amount of lurbinectedin. Bars represent the
743 averages ± SEM of the percentage of cells with one or more Rad52 foci from 3
744 independent experiments. Statistical significance was assessed by Student's t-
745 test.
746

Figure 1

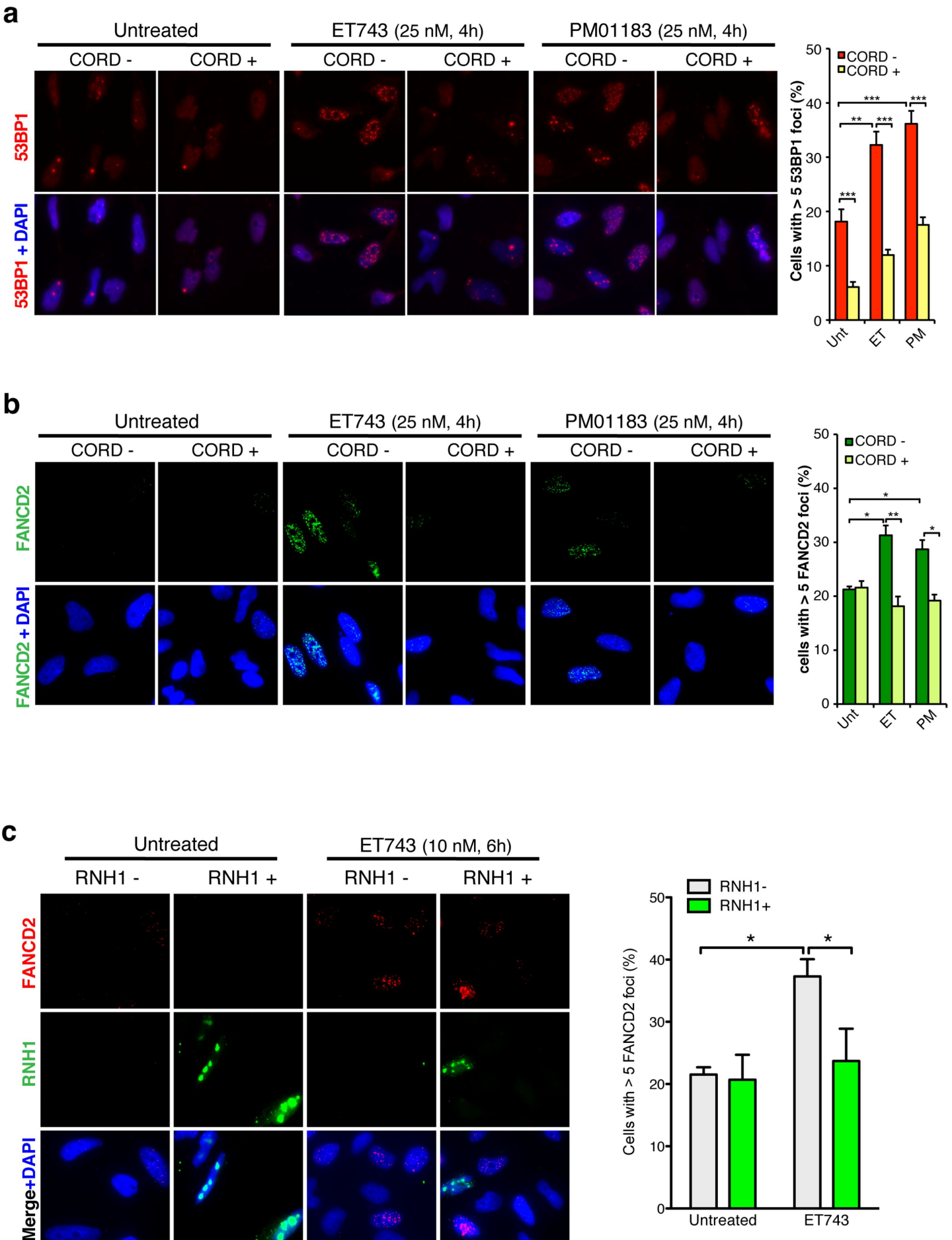
a
Untreated
ET743 (25 nM, 4h)
PM01183 (25 nM, 4h)
CORD -
CORD +
53BP1
53BP1 + DAPI
Cells with > 5 53BP1 foci (%)
Unt
ET
PM
b
FANCD2
FANCD2 + DAPI
cells with > 5 FANCD2 foci (%)
c
Untreated
ET743 (10 nM, 6h)
RNH1 -
RNH1 +
FANCD2
RNH1
Merge+DAPI
RNH1-
RNH1+
Cells with > 5 FANCD2 foci (%)
Untreated
ET743

Figure 2

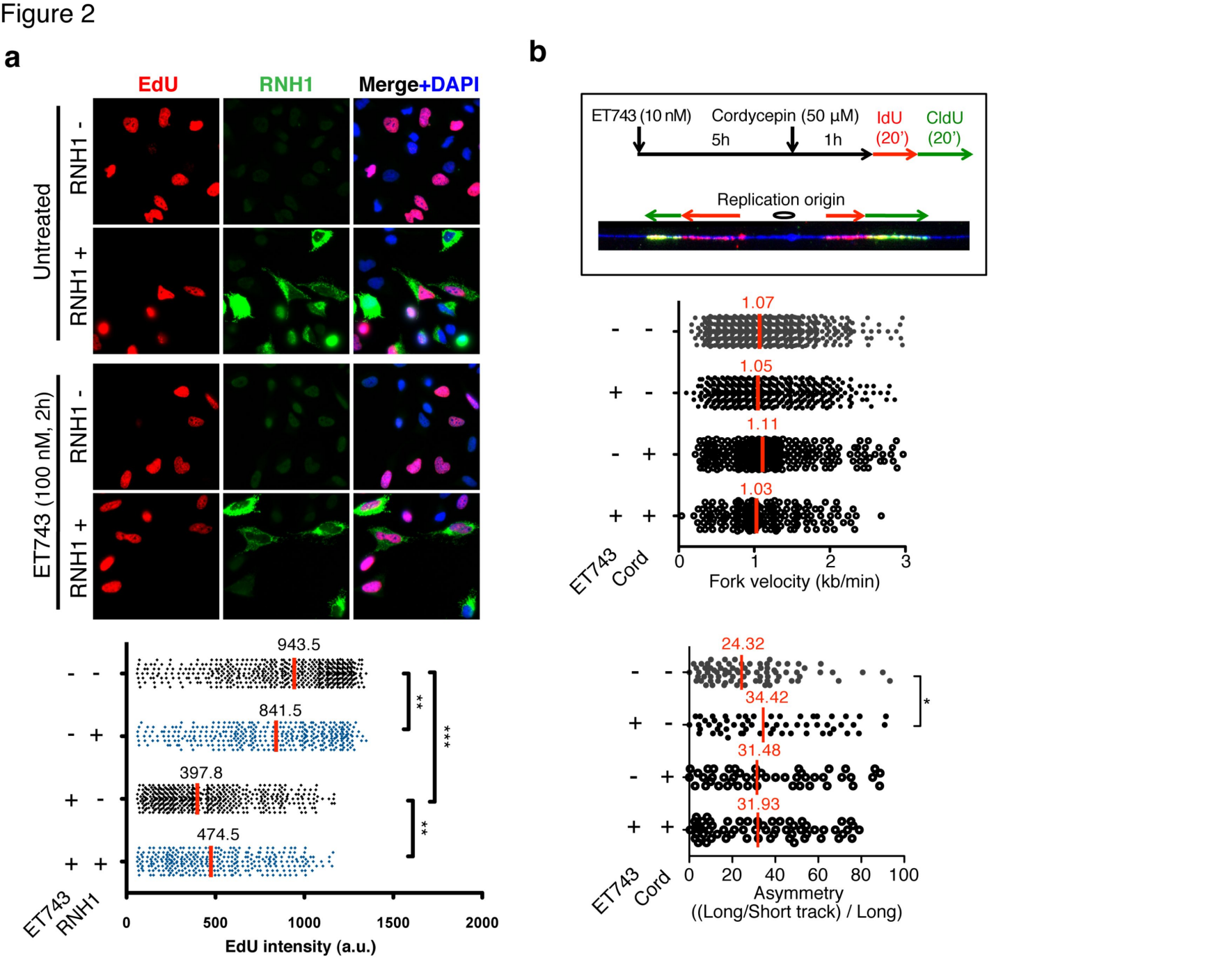
a
EdU
RNH1
Merge+DAPI
Untreated
RNH1 -
RNH1 +
ET743 (100 nM, 2h)
RNH1 -
RNH1 +
943.5
841.5
397.8
474.5
**
***
**
ET743
RNH1
0
500
1000
1500
2000
EdU intensity (a.u.)
b
ET743 (10 nM)
Cordycepin (50 µM)
5h
1h
IdU (20')
CldU (20')
Replication origin
1.07
1.05
1.11
1.03
ET743
Cord
0
1
2
3
Fork velocity (kb/min)
24.32
34.42
31.48
31.93
*
ET743
Cord
0
20
40
60
80
100
Asymmetry
((Long/Short track) / Long)

Figure 3

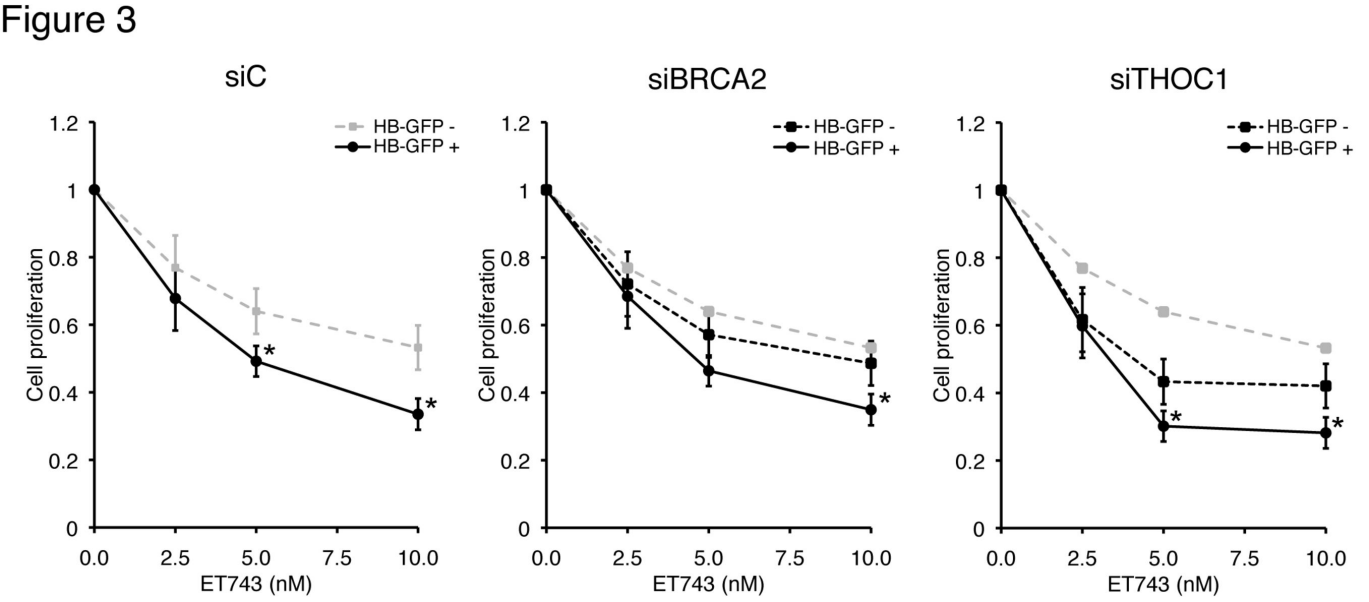
siC
siBRCA2
siTHOC1
HB-GFP -
HB-GFP +
Cell proliferation
ET743 (nM)
0
0.2
0.4
0.6
0.8
1
1.2
0.0
2.5
5.0
7.5
10.0
*

Figure 4

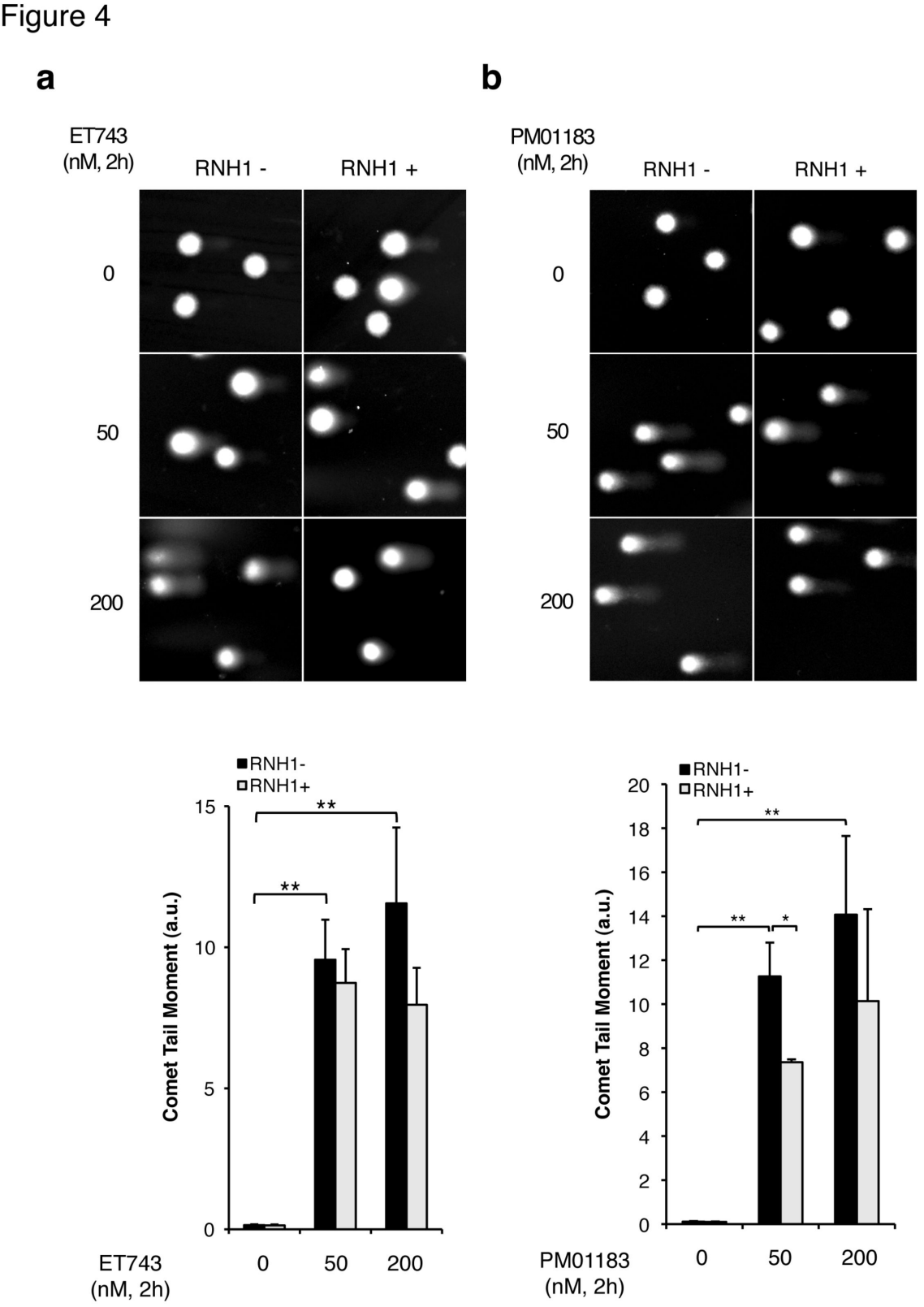
a
b
ET743
(nM, 2h)
RNH1 -
RNH1 +
0
50
200
PM01183
(nM, 2h)
RNH1 -
RNH1 +
0
50
200
RNH1-
RNH1+
Comet Tail Moment (a.u.)
15
10
5
0
**
**
ET743
(nM, 2h)
0
50
200
RNH1-
RNH1+
Comet Tail Moment (a.u.)
20
18
16
14
12
10
8
6
4
2
0
**
**
*
PM01183
(nM, 2h)
0
50
200

Figure 5

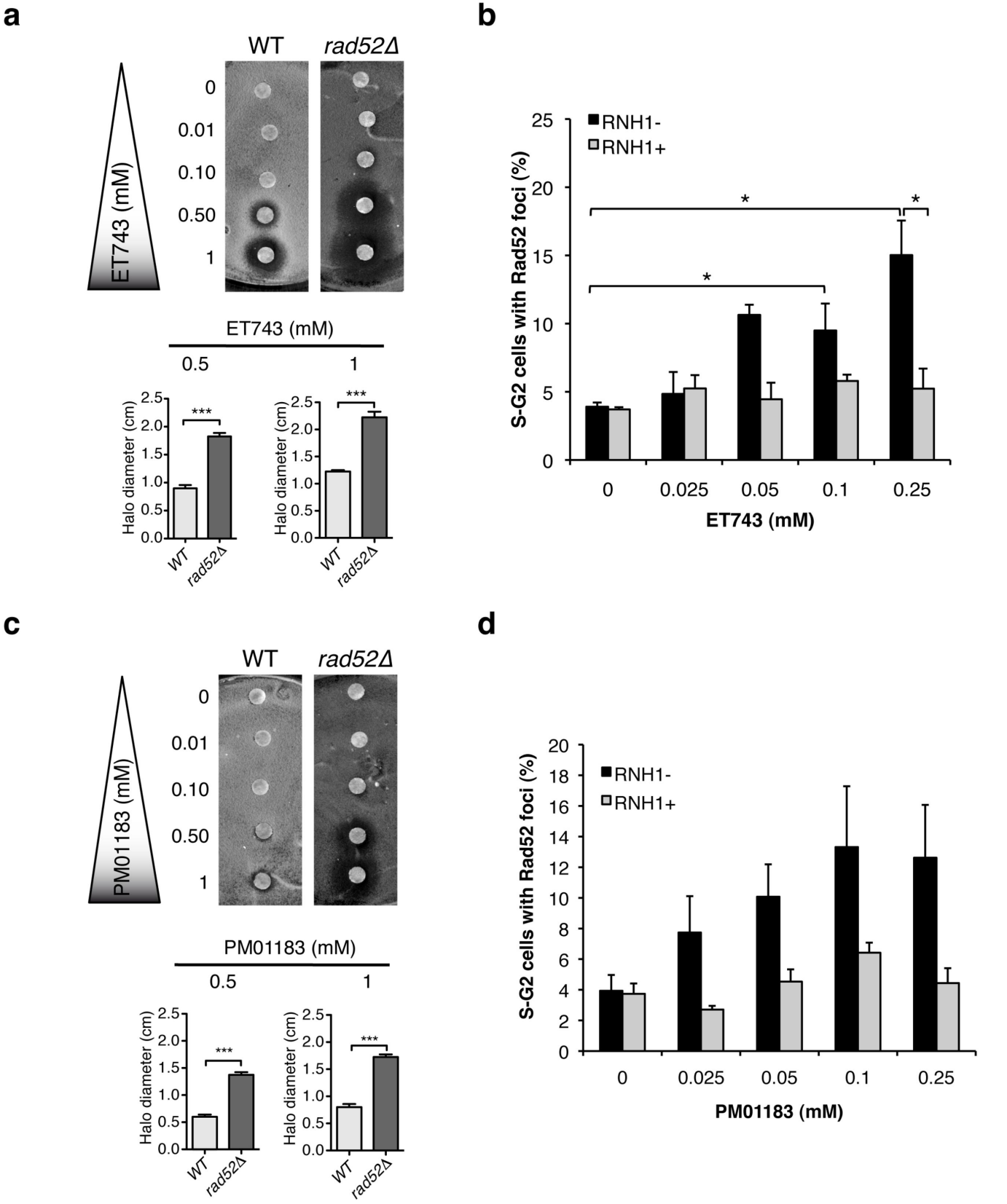
a
WT
rad52Δ
ET743 (mM)
0
0.01
0.10
0.50
1
ET743 (mM)
0.5
1
Halo diameter (cm)
***
WT
rad52Δ
b
RNH1-
RNH1+
S-G2 cells with Rad52 foci (%)
*
*
0
0.025
0.05
0.1
0.25
ET743 (mM)
c
WT
rad52Δ
PM01183 (mM)
0
0.01
0.10
0.50
1
PM01183 (mM)
0.5
1
Halo diameter (cm)
***
WT
rad52Δ
d
RNH1-
RNH1+
S-G2 cells with Rad52 foci (%)
0
0.025
0.05
0.1
0.25
PM01183 (mM)